Available online at www.sciencedirect.com

ScienceDirect

IFAC Papers Online CONFERENCE PAPER ARCHIVE

IFAC PapersOnLine 51-15 (2018) 1062–1067

Joint structure for the real-time estimation and control of automotive dry clutch engagement

Mojtaba Sharifzadeh * **Mario Pisaturo** * **Arash Farnam** ** **Adolfo Senatore** *

* *Department of Industrial Engineering, University of Salerno, Italy. (e-mail: {msharifzadeh, mpisaturo, asenatore}@unisa.it)*

** *Data Science Lab, Faculty of Engineering and Architecture, Ghent University, Ghent, Belgium. (e-mail:arash.farnam@ugent.be)*

Abstract:
In this paper, real-time identification of the dry-clutch torque characteristics model in automotive systems is investigated. The proposed algorithm focused to provide the direct capability to update the clutch torque characteristics model by using engine speed and torque as measurable signals in real-time, within a multiple model predictive control loop. First, the clutch torque is estimated with some uncertainty. Then, it is proposed a new trust-region based identification approach which is robust enough to cover this uncertainty. The aim of the MPC controller is to ensure a comfortable lockup by avoiding engine stall and reasonable engagement time. The effectiveness and performance of the approach are demonstrated through the real-time model simulations in various conditions.

Keywords: Vehicle dynamics, recursive estimation, dry-clutch torque

1. INTRODUCTION

Since the electro-actuated clutch in Automated Manual Transmissions (AMTs) plays a key role in today's vehicle industry, it is necessary to have a robust identification of automotive dry clutch system parameters for improving control performance (Senatore et al., 2017; Fredriksson and Egardt, 2003). As well known, AMTs are directly derived from manual ones through the integration of actuators; then, development and production costs are generally lower than other automatic transmissions, while the reliability and durability are at highest level. Several models of control strategies for dry clutches in AMTs have been recently proposed in the literature in order to attain reduction of fuel consumption and pollutant emissions, lower gearshift time, decrease of facing wear, and increase of comfort. The parameters of clutch transmission model need to be estimated in order to satisfy the above stated objectives along with small friction losses, minimum time needed for the adaptive control of the engagement, time delay stability problem, improvement of driver and passengers comfort, fast jerk-free gearshifts (Garofalo et al., 2002; Sharifzadeh et al., 2018). Therefore, it is necessary to design real-time estimation scheme based on the available system. In (Arndt et al., 2016) the Levenberg-Marquardt method (LM) is used to estimate the parameters. Since it is non-recursive identification approach, it can not be easily adapted in real-time variations. On the other hand, recursive methods for nonlinear optimization can be classified into line search methods and trust region methods. Trust region methods are robust and give faster convergence rate for minimizing vector-function with large number of elements. They can be applied to broad range of dynamic problems in mechanical systems and automotive devices. In this paper, a novel identification approach of frictional torque of dry-clutch automotive system is introduced. In this algorithm, first clutch torque is estimated. Then it is used for the identification of incipient sliding point (ISP) also called the "kiss-point" of throwout bearing, whose knowledge has strong influence on clutch transmitted torque in order to improve engagement performance of gearbox control system. Thus, considering that we have noisy estimated clutch torque data, an interior Trust-Region method is applied to kiss-point identification procedure. The main novelty of this joint structure is the rule that it allows the current time-slot to be processed and considers future time-slots simultaneously. Model Predictive Control (MPC) uses the current dynamic state of the system, the current plant measurements and the process variable targets and limits to calculate future changes in the dependent variables considering the continuous update of reference signals.

Since the MPC control unit, sends only the first change in each independent variable to be implemented, and repeats the process when the next change is required, it could process only when there is an updated clutch data in the recursion and this speeds up the process. Example of vehicle dynamics and active driveline control could be also found in (Terzo and Timpone, 2013; De Simone and Guida, 2018a). The coupling between controller role and dynamic stability behavior of mechanical system with friction has been analyzed in (De Simone and Guida, 2018b), whereas simulation of evolution in time of multibody system under frictional actions and restrictions imposed by the kine-

10.1016/j.ifacol.2018.09.053

matic joints is investigated in (Pappalardo and Guida, 2017).

2. SYSTEM DESCRIPTION

In this section, modeling and system descriptions of both dry clutch engagement process and driveline system is presented. A dry-clutch engagement system consists of a steel clutch disc connected to a hub by means of torsional damper springs which damp out torsional vibrations (Pica et al., 2016). The paddles and two or more friction pads (also called the clutch facings) are clamped to the clutch disc with rivets. A diaphragm spring (or a washer spring or a Belleville spring) is clamped to the cover and to the pressure plate (or the push plate). The latter three parts are torsionally clamped to the flywheel while the clutch disc is torsionally clamped to the main shaft. The diaphragm spring transforms the throwout bearing position x_{to} into a corresponding pressure plate position x_{pp}. The pressure plate presses the clutch disc against the flywheel or keeps it apart. The friction between the external pads on the two sides of the clutch disc and the flywheel and pressure plate respectively generates the torque transmitted from the engine to the driveline through the clutch. When the pressure plate and the clutch disc have the same speed as the flywheel because they are constrained by the diaphragm spring, the clutch is locked up. In such operating conditions the engine is directly connected to the driveline. Therefore the cushion spring (also called the flat spring) is compressed and, when it is completely compressed, the clutch is closed. Conversely, when the pressure plate position is such that the cushion spring is not compressed, the clutch is open. When the clutch is going from open to locked up, it is in the engagement phase.

The cushion spring is a thin wavy steel disc placed between the clutch friction pads and is designed with different radial stiffnesses in order to ensure the desired smoothness of engagement. Knowledge of the clutch engagement scheme allows correlation of the throwout bearing displacement, the cushion spring compression and the clutch torque transmissibility (Cappetti et al., 2012).

The throwout bearing position x_{to} is the clutch variable directly controlled by the TCU through the electrohydraulic actuator, and its position results in the given pressure plate position and cushion spring deflection. When $x_{to} = 0$, the clutch is open, when $x_{to} = x_{to}^{cnt}$, the friction pad and flywheel come into contact (also called the kiss-point) and, when $x_{to} \in \left[x_{to}^{cls}, x_{to}^{max}\right]$ the clutch is closed.

In (Vasca et al., 2011), a novel model of dry-clutch torque transmissibility based on throwout bearing motion and ensuing compression of the cushion spring is proposed. The clutch torque proposed in that work is given by

$$T_{fc} = nR_{\mu}F_{fc}(x_{to}) \tag{1}$$

where n is the number of the pairs of contacts (n = 2 in our case), R_{μ} is a coefficient (function) taking into account the dynamic friction phenomenon, $F_{fc}(x_{to})$ is the axial reaction of the cushion spring which is formulated as below,

$$F_{fc}(x_{to}) = \check{F}.\left(1 - \sqrt{1 - \left(\frac{x_{to} - x_{to}^{cnt}}{x_{to}^{cls} - x_{to}^{cnt}}\right)^2}\right) \tag{2}$$

$$R_{\mu}(\omega_{fc}) = \check{R}sat(\check{\mu} - \check{\beta}\omega_{fc}) \tag{3}$$

where $\check{R}$ is the equivalent radius of the friction surfaces, $\check{F}$ is the maximum axial reaction of the cushion spring and $\omega_{fc} = \omega_f - \omega_c$ is the slip speed, with the subscripts e, f, c, g, d, w indicate engine, flywheel, clutch disc, gearbox, differential and wheels, respectively. where T indicates the torques, J the inertias and b the damping coefficients.

The scheme of the analysed driveline under the hypothesis that all shafts are rigid as well as gears are ideal, i.e. $\omega_w = \frac{\omega_c}{r_1 r_d}$, and the related equations are (Pisaturo et al., 2015a):

$$J_{ef}\dot{\omega}_e = T_e - b_e\omega_e - T_{fc} \tag{4}$$

$$J_v\dot{\omega}_w = r_1 r_d T_{fc} - b_g\left(r_1 r_d\right)^2\omega_w - T_w \tag{5}$$

where r_1 and r_d are the gear ratios on the engine side and differential respectively. Under the assumption that synchronizer dynamics can be neglected. In addition, the following positions hold:

$$J_{ef} = J_e + J_f \tag{6}$$

$$J_v = J_w + J_d + \left(J_{g2}\right)r_d^2 + \left(J_{g1} + J_c\right)\left(r_1 r_d\right)^2 \tag{7}$$

$$T_w = mgR_w\left(\sin(\phi) + f\cos(\phi)\right) + \\ + \frac{1}{2}\rho_{aria}AC_x v^2 R_w + T_{brake} \tag{8}$$

where, m is the vehicle mass, R_w is the wheel radius, ϕ is the road slope, f is the rolling resistance coefficient, ρ_{aria} is the air density, A is the vehicle frontal area, C_x is the air drag coefficient, v the vehicle speed and T_{brake} is the braking torque.

The equation which represents the "locked-up" model can be derived from eqs. (4) and (5) by taking into account driveline dynamics reduced to engine (or wheel) side. For control purpose the state-space representation is a useful alternative mathematical representation of the driveline (Pisaturo et al., 2015a,b).

3. CONTROLLER DESIGN

In this section the model predictive control (MPC) approach is explained. The MPC has been designed with the discrete time version of the driveline model. A sampling time of 0.01 s and the zero-order hold method have been used to discretize the state-space equations. This value is compatible for automotive applications (Quanan et al., 2011).

As explained above, the driveline could operate in two different working conditions: the slipping phase and the engaged phase. It is worth noting that both the state matrices and input matrices change by changing the gear ratio r_1. Conversely from (Pisaturo et al., 2015a,b), in

this paper only one controller has been implemented but the penalty weights are time-variant accordingly with working conditions. In this way the memory demand in the transmission control unit (TCU) is lower because it is not necessary to store different controllers but only different weights. On the other hand, is also true that the controller has been designed only for the start-up phase so it is not optimized for the gear-shifts phases, i.e. with different gear ratio. But this choice can be justified because the aim of this paper is to analyse only the launch manoeuvre. The state-space representation used to design the MPC is reported below:

$$\begin{cases} \mathbf{x}_{k+1} = \bar{\mathbf{A}}\mathbf{x}_k + \bar{\mathbf{B}}\mathbf{u}_k \\ \mathbf{y}_k = \bar{\mathbf{C}}\mathbf{x}_k \end{cases} \tag{9}$$

where $\mathbf{x} = \mathbf{y} = [\omega_e \ \omega_w]^T$ are the state and output vectors and $\mathbf{u} = [T_e \ T_{fc} \ T_w]^T$ is the input vector. To design the controller it has been assumed that ω_e and ω_w are measured output. Moreover, T_e and T_{fc} are manipulated variables whereas T_w is a measured disturbance. Finally, the default Matlab MPC Toolbox with a prediction horizon of 10 time steps and a control horizon of 3 time steps have been used to carry out the simulations (Morari and Ricker, 1998).

3.1 Constraints

Some constraints both on the "plant" input and output have been imposed to design the MPC to avoid the engine stall condition and guarantee comfortable lock-up.

On the "plant" input saturation constraints have been imposed both on the torques and on their variation rates:

$$T_e \in \left[T_e^{\min}, T_e^{\max}\right] \tag{10}$$

$$T_{fc} \in \left[T_{fc}^{\min}, T_{fc}^{\max}\right] \tag{11}$$

$$\dot{T}_e \in \left[\dot{T}_e^{\min}, \dot{T}_e^{\max}\right] \tag{12}$$

where $T_e^{\min} = -73 \ Nm$ is the minimum engine torque value, $T_e^{\max} = 320 \ Nm$ is the maximum engine torque value, $T_{fc}^{\min} = 0 \ Nm$ is the minimum torque value transmitted by the clutch, $T_{fc}^{\max} = 425 \ Nm$ is the maximum torque value that the clutch can transmit, $\dot{T}_e^{\min} = -20 \ Nm/s$ is the maximum decrease (≤ 0) in one step and $\dot{T}_e^{\max} = 20 \ Nm/s$ is the maximum increase (≥ 0) in one step to take into account the engine torque build-up phenomenon.

Instead, on the "plant" outputs, engine and clutch angular speeds, the following constraints hold:

$$\omega_e \in \left[\omega_e^{kill}, \omega_e^{\max}\right] \tag{13}$$

$$\omega_c \geq \omega_c^{\min} \tag{14}$$

where $\omega_e^{kill} = 60 \ rads^{-1}$ represents the so-called no-kill condition (Glielmo et al., 2006), $\omega_e^{\max} = 600 \ rads^{-1}$ is the maximum value of the engine speed before attaining critical conditions and $\omega_c^{\min} = 0 \ rads^{-1}$ is the minimum value of clutch speed during the vehicle launch. Superscript kill stands for the condition with minimum speed of the engine assumed as threshold of engine switch off, whereas superscript max stands for the condition of overrunning engine speed as threshold of engine limiter trigger.

3.2 Optimization problem and tuning

The goal of the optimization problem is to minimize a cost function while satisfying constraints each time step. In particular, it takes into account four different, and sometime conflicting, aspects.

$$\begin{aligned} J = &[\mathbf{y}_j - \mathbf{r}_j]^T \mathbf{W}_{y,j}^2 [\mathbf{y}_j - \mathbf{r}_j] + ... \\ &+[\mathbf{u}_i - \mathbf{u}_{\text{target},i}]^T \mathbf{W}_{u,i}^2 [\mathbf{u}_i - \mathbf{u}_{\text{target},i}] + ... \\ &+\Delta\mathbf{u}_i^T \mathbf{W}_{\Delta u,i}^2 \Delta\mathbf{u}_i + \rho_\varepsilon \varepsilon^2 \end{aligned} \tag{15}$$

where: $\mathbf{u}_i = [\, u_i(0) \ ... \ u_i(P-1) \,]^T$ is the input vector;

$\mathbf{u}_{\text{target},i} = [\, u_{\text{target,i}}(0) \ ... \ u_{\text{target,i}}(P-1) \,]^T$ is the input target vector; $\Delta\mathbf{u}_i = [\, \Delta u_i(0) \ ... \ \Delta u_i(P-1) \,]^T$ is the input increment vector;

$\mathbf{y}_j = [\, y_j(1) \ ... \ y_j(P) \,]^T$ is the output vector;

$\mathbf{r}_j = [\, r_j(1) \ ... \ r_j(P) \,]^T$ is the reference trajectory vector;

$\mathbf{W}_{u,i}$, $\mathbf{W}_{\Delta u,i}$ and $\mathbf{W}_{y,j}$ are, respectively, the input, input increment and output scaled weights matrices (diagonals and squares). Finally, the subscript i and j take into account the *ith* inputs and *jth* outputs of the "plant" respectively. The controller aims to keep plant outputs as close as possible the reference signals. Also the manipulated variables, i.e. plant inputs, must be the closest possible their target values by avoiding large fluctuations in one step. Finally, to prevent infeasible QP solution a dimensionless non-negative slack variable is introduced in the cost function by softening some constraints. For this reason a tuning procedure of some controller parameters is necessary. The parameters to be tuned are the prediction horizon P, the control horizon m, the input, input increments and output scaled weights matrices $W_{u,i}$, $W_{\Delta u,i}$, $W_{y,j}$ respectively, and overall penalty weight ρ_ϵ. As mentioned before, a prediction horizon of 10 time steps and a control horizon of 3 time steps with the sampling time of 0.01 s has been chosen. The following facts are remarkable for the stability of the scheme: the MPC has been designed by considering the driveline dynamics described by eqs. (4) and (5) and for discrete state-space representation it is described by the equation (9). The only non-linearities in these equations are the plant inputs: the engine torque T_e, clutch torque T_{fc} and the wheel load torque T_w (measured disturbance); they have been implemented through static maps (look-up tables) based on phenomenological models outside from the MPC. In this way they have not been taken into account to design the MPC. Moreover, in this work only the vehicle launch phase has been analyzed: in such a way the gear ratio is constant and this allows constant state matrix A, input matrix B and output matrix C. The parameters to be tuned are the prediction horizon, the control horizon, the input, output and input increments and the overall penalty weight. The tuning procedure has been proven to be effec-

tive according to typical time scale of launch maneuver, actuator dynamics and plant disturbance (Pisaturo et al., 2016; Myklebust and Eriksson, 2015). The driving criteria adopted to select these parameters are a trade-off between fast engagement and comfortable lock-up. In particular, this goal is easily achievable by a suitable choice of the weights. Instead, the prediction and the control horizon, together with the inputs weights, allow the steady-state solution to be improved.

4. IDENTIFICATION

Since, good choice of the MPC control parameters allows better performance in terms of safety of the system and comfortable engagement process, in this section a new identification algorithm is designed to update the kiss-point value. As it is clear in equation (16), the robust identification of the kiss-point x_{to}^{cnt} is achievable by estimating clutch torque and using its model in real-time environment. x_{to}^{cnt} is a functional to improve the inversion of clutch torque characteristic to properly drive the clutch actuator (Fig. 4). It is attainable by minimizing the estimation error $er(x_{to}^{cnt}) = T_{fc}^{a}(x_{to}, x_{to}^{cnt}) - \hat{T}_{fc}^{b}(T_e, \omega_e)$.

$$\begin{cases} T_{fc}^{a}(x_{to}, x_{to}^{cnt}) = nR_{\mu}\check{F}.\left(1 - \sqrt{1 - \left(\frac{x_{to} - x_{to}^{cnt}}{x_{to}^{cls} - x_{to}^{cnt}}\right)^2}\right) \\ \hat{T}_{fc}^{b}(T_e, \omega_e) = T_e(t) - b_e\omega_e(t) - J_{ef}\dot{\omega}_e(t) \end{cases} \quad (16)$$

Iterative methods for nonlinear optimization can be classified into line search methods and trust region methods. Trust region methods are robust and give faster convergence rate for vector-function with uncertainty (Sharifzadeh et al., 2016). Thus, considering that noisy data comes from the estimated clutch torque, in order to solve the above subproblem an interior Trust-Region method, is utilized in the present work.

$$\text{minimize } er(x_{to}^{cnt}) \text{ subject to } x_{to}^{cnt} \in [l_{lo}, l_{up}], \quad (17)$$

Assuming that the first and second derivatives of er are all continuous in a neighborhood D_f, the quadratic approximation can be defined by the first two terms of local Taylor expansion of $er(x_{to}^{cnt})$ at x_{to}^{cnt} , i.e.,

$$er(x_{to}^{cnt}+s) \approx er(x_{to}^{cnt}) + \underbrace{s^T\nabla er(x_{to}^{cnt}{}_k) + \frac{1}{2}s^T\nabla^2 er(x_{to}^{cnt}{}_k)s}_{\psi_k(s)} \quad (18)$$

which yields to

$$\begin{array}{l} \underset{s\in\Re^N}{min} \quad s^T g_k + \frac{1}{2}s^T H_k s = \psi_k(s) \\ such\ that\ \|s\|_2 \le \mathbf{R}_k, \end{array} \quad (19)$$

where $g_k = \nabla er(x_{to}^{cnt}{}_k)$ is the gradient at the current iteration, $H_k = \nabla^2 er(x_{to}^{cnt}{}_k)$ is symmetric matrix denotes the Hessian of $er(x_{to}^{cnt})$ and $\mathbf{R}_k > 0$ is a trust region radius. The standard form $\psi_k(s)$ is a scalar function which can be easily solved with computational optimization methods. That is to say $\psi_k(s)$ is a model of reduction in er within the neighborhood of iterate $x_{to}^{cnt}{}_k$. This suggests that it may be desirable to calculate Trust-Region step s_k which solves subproblem (19). Now $x_{to}^{cnt}{}_k$ can be updated by 8.2 (see algorithm 1).

As it is pointed in step 8.3 (algorithm 2) if updating term $x_{to}^{cnt}{}_{k+1} = x_{to}^{cnt}{}_k + s_k$ produces a sufficient reduction in er, then $\mathbf{R}_k$ can be increased; else if it doesn't satisfy the acceptable range of reduction then $\mathbf{R}_k$ should be decreased.

The convergent solution is achieved after only about 7 iterations. The proposed identification method for the clutch torque transmission system is summarized in algorithm 1. This joint structure allows the current time-slot to be processed and considers future time-slots simultaneously.

Algorithm 1 Proposed recursive algorithm for this problem

1: Initialisation of the parameters
2: **repeat**
3: Update $T_e(t)$ and $\omega_e(t)$ values from the Engine Control Unit (ECU)
4: Estimate noisy $\hat{T}_{fc}^{b}(T_e, \omega_e)$ using $\hat{T}_{fc}^{b}(T_e, \omega_e) = T_e(t) - b_e\omega_e(t) - J_{ef}\dot{\omega}_e(t)$
5: Determine the $T_{fc}^{a}(x_{to}, x_{to}^{cnt})$ using equations (16)
6: Calculate $er(x_{to}^{cnt}) = T_{fc}^{a}(x_{to}, x_{to}^{cnt}) - \hat{T}_{fc}^{b}(T_e, \omega_e)$
7: Given $\mathbf{R}_1 > 0$ let $k = 1$,
8: **while** (Not converged) **do**
9: 8.1) Solve subproblem (19) giving s_k
10: 8.2) Update $x_{to}^{cnt}{}_k$, i.e.

$$x_{to}^{cnt}{}_{k+1} = \begin{cases} x_{to}^{cnt}{}_k \text{ if } \begin{array}{l} er(x_{to}^{cnt}{}_k) \le er(x_{to}^{cnt}{}_k + s_k) \\ \textbf{or} \quad x_{to}^{cnt}{}_k + s_k \notin [l_{lo}, l_{up}] \end{array} \\ x_{to}^{cnt}{}_k + s_k \quad \text{otherwise,} \end{cases} \quad (20)$$

11: 8.3) Trust region radius update. Set

$$r_k = \left(er(x_{to}^{cnt}{}_k) - er(x_{to}^{cnt}{}_k + s_k)\right)/\psi_k(s_k),$$

$$\mathbf{R}_{k+1} \in \begin{cases} [.25\,\|s_k\|_2\,,\ .5\mathbf{R}_k] & if\ r_k < .25, \\ [\mathbf{R}_k,\ 2\mathbf{R}_k] & otherwise; \end{cases}$$

12: 8.4) Update g_k, H_k *and* $k = k + 1$
13: **end while**
14: Update inputs
15: **until** (there are no more input data available)

Let $er(x_{to}^{cnt}{}_k) : \Re^n \to \Re$ is twice differentiable and bounded below on $\Re^n$. Assume that there exists a bounded convex closed set $\Omega \subset \Re^n$ such that $x_{to}^{cnt}{}_k$ are in Ω for all k . Also note that $\nabla^2 er(x_{to}^{cnt*}{}_k)$ is assumed to be nonsingular where $x_{to}^{cnt*}{}_k$ is a limit point of $\{x_{to}^{cnt}{}_k\}$. Considering the assumption which was made above, asymptotic convergence of the method is guaranteed and the process is completely identifiable (see Sharifzadeh et al. (2017)).

5. SIMULATION RESULTS

The estimation of dry-clutch torque transmission conditions is one of the applications that can benefit most from the presented NLLS identification algorithm. To highlight this fact, this section presents simulation results to validate the proposed structure in estimating the kiss-point value in real-time considering MPC control structure. The simulation is performed under several different steps. Since the constant parameters of dry-clutch do not show considerable differences for our purpose, average value of them are considered to evaluate the algorithm. In this work at the first step, we focused on the equation (16) in order to

perform the estimation. As said before, estimating the kiss-point value is crucial to update the clutch torque model in the clutch engagement control loop.

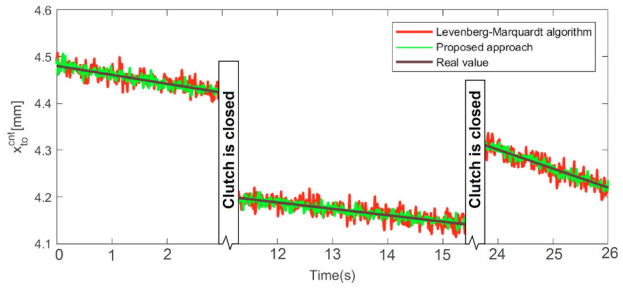

Fig. 1. Estimation of the kiss-point during iterations

Figs 1, 2, and 3 show the estimation of the x_{to}^{cnt} for three engagements for vehicle launch and gearshift in few seconds. In order to consider more realistic settings, the simulations have been done by noisy data. Figure 1 shows the results when there is a zero mean white noise with $\sigma^2_{T_{fc}} = 4.0943N^2m^2$ in the estimated data and demonstrates the estimation convergence during iterations of the algorithm. In the Figure 2 zero mean white noise with $\sigma^2_{x_{to}^{cls}} = .002mm^2$ is added to the x_{to}^{cls}.

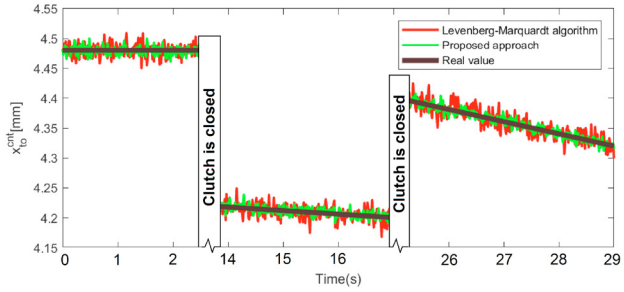

Fig. 2. Estimation of the kiss-point during different engagements

The simulation result considering the both uncertainties with $\sigma^2_{T_{fc}} = 2.031N^2m^2$ and $\sigma^2_{x_{to}^{cls}} = .001mm^2$ is shown in the figure 3. The simulations for the Figs 1, 2, and 3 are performed for the worst case initial value as well as considering mentioned uncertainties which results the convergence in 6, 6 and 8 iterations respectively. Two different approaches are considered for the problem. Both the well known Levenberg-Marquardt algorithm and the proposed algorithm are applied to perform the estimation problem. As it is demontrated from the results, the proposed algorithm shows better results than the Levenberg-Marquardt algorithm.

The scheme of the proposed joint structure is shown in the Figure 4. As it is shown, estimation and control units are considered in the closed loop. It is clear that the proposed identification approach is robust enough to update the x_{to}^{cnt} value which is needed for the MPC control unit, considering that there is significant uncertainty in the estimated value of the clutch torque.

The figures 5 and 6 show the results of a launch maneuver for the total structure described above. Fig. 5 shows the plots of the engine and the clutch torques. The solid black line represents the set point T_{fc} and dashed blue line and

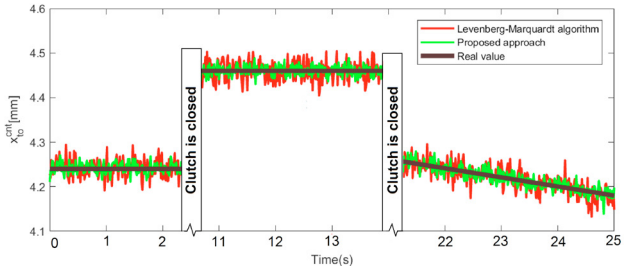

Fig. 3. Estimation of the kiss-point during different engagements in real scale

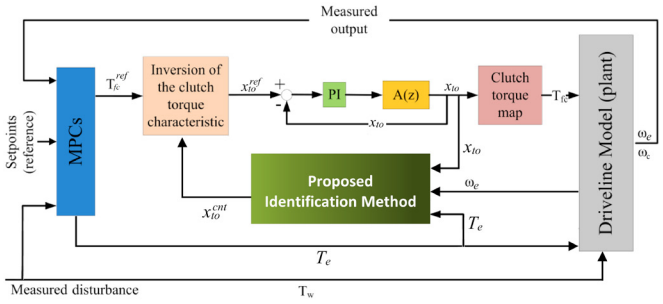

Fig. 4. Implementation of the proposed joint structure

dash-dot red lines represent the T^b_{fc} and the T_{eng}, respectively. Note that the torque estimation is considered during slipping phase. After that engaged condition is attained, the throwout bearing position reaches its maximum value, corresponding the maximum torque transmittable by the clutch by considering the frictional map and the cushion spring characteristics.

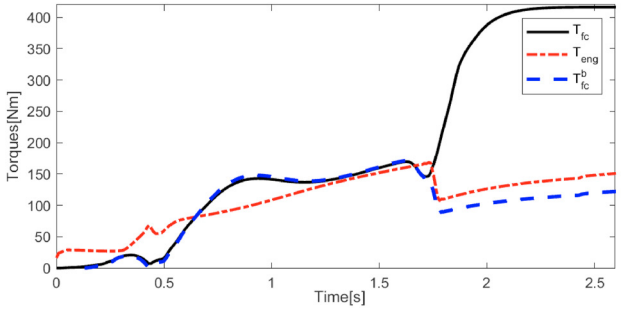

Fig. 5. Clutch and engine Torques vs.time

Fig. 6 shows the plots of the engine and the clutch angular speeds which demonstrates good results for the MPC controller based on clutch torque characteristics model identification. The solid red line represents the set point ω^{ref}_{clutch} respectively. The dashed black line and blue line represent the angular speeds for the engine and the clutch, respectively.

6. CONCLUSIONS

In this work, new real-time joint structure with clutch torque characteristics model identification algorithm and multiple MPC for dry clutch engagement problem during vehicle launch has been proposed. First, clutch torque is estimated with some uncertainty, using engine torque and engine angular speed in real-time. Then the torque transmission model based on the relation between clutch torque

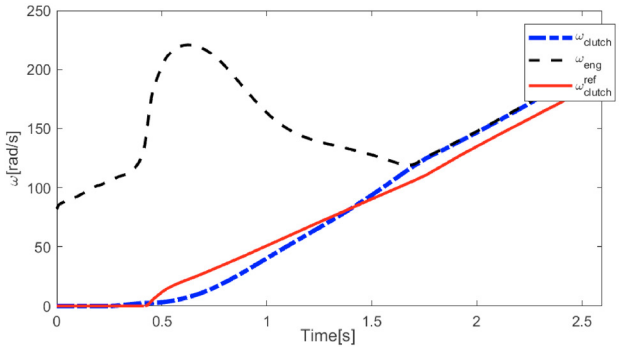

Fig. 6. Clutch and engine angular speeds vs. time

and throwout bearing position is considered to identify the kiss-point value. The estimated value is considered to update the MPC controller parameters. In order to have more comfortable engagement process, a new MPC controller for the slipping phase has been designed. The effectiveness of proposed algorithms are demonstrated through simulations. Further investigation will deal with clutch torque estimation based on measurements on test vehicle. The estimation will apply the methodology explained in this paper to estimate clutch torque evolution during repeated launch maneuvers in a compact passenger car.

REFERENCES

Arndt, T., Tarasow, A., Bohn, C., Wachsmuth, G., and Serway, R. (2016). Estimation of the clutch characteristic map for wet clutch transmissions considering actuator signal and clutch slip. *IFAC-PapersOnLine*, 49(11), 742–748.

Cappetti, N., Pisaturo, M., and Senatore, A. (2012). Modelling the cushion spring characteristic to enhance the automated dry-clutch performance: The temperature effect. *Proceedings of the Institution of Mechanical Engineers, Part D: Journal of Automobile Engineering*, 226(11), 1472–1482.

De Simone, M.C. and Guida, D. (2018a). Identification and control of a unmanned ground vehicle by using Arduino. *UPB Sci. Bull. Ser. D*, 80, 141–154.

De Simone, M.C. and Guida, D. (2018b). Modal coupling in presence of dry friction. *Machines*, 6(1), 8.

Fredriksson, J. and Egardt, B. (2003). Active engine control for gearshifting in automated manual transmissions. *International journal of vehicle design*, 32(3-4), 216–230.

Garofalo, F., Glielmo, L., Iannelli, L., and Vasca, F. (2002). Optimal tracking for automotive dry clutch engagement. *IFAC Proceedings Volumes*, 35(1), 367–372.

Glielmo, L., Iannelli, L., Vacca, V., and Vasca, F. (2006). Gearshift control for automated manual transmissions. *IEEE/ASME transactions on mechatronics*, 11(1), 17–26.

Morari, M. and Ricker, N.L. (1998). *Model predictive control toolbox: for use with MATLAB*. MathWorks Incorporated.

Myklebust, A. and Eriksson, L. (2015). Modeling, observability, and estimation of thermal effects and aging on transmitted torque in a heavy duty truck with a dry clutch. *IEEE/ASME transactions on mechatronics*, 20(1), 61–72.

Pappalardo, C.M. and Guida, D. (2017). On the use of two-dimensional Euler parameters for the dynamic simulation of planar rigid multibody systems. *Archive of Applied Mechanics*, 87(10), 1647–1665.

Pica, G., Cervone, C., Senatore, A., Lupo, M., and Vasca, F. (2016). Dry dual clutch torque model with temperature and slip speed effects. *Intelligent Industrial Systems*, 2(2), 133–147.

Pisaturo, M., Cirrincione, M., and Senatore, A. (2015a). Multiple constrained MPC design for automotive dry clutch engagement. *IEEE/ASME Transactions on Mechatronics*, 20(1), 469–480.

Pisaturo, M., D'Auria, C., and Senatore, A. (2016). Friction coefficient influence on the engagement uncertainty in dry-clutch AMT. In *American Control Conference (ACC), 2016*, 7561–7566. IEEE.

Pisaturo, M., Cirrincione, M., and Senatore, A. (2015b). Influence of the temperature on the dry-clutch engagement control in gear-shift manoeuvres. In *Control and Automation (MED), 2015 23th Mediterranean Conference on*, 109–116. IEEE.

Quanan, H., Jian, S., and Lei, L. (2011). Research on rapid testing platform for TCU of automated manual transmission. In *Measuring Technology and Mechatronics Automation (ICMTMA), 2011 Third International Conference on*, volume 3, 67–70. IEEE.

Senatore, A., Pisaturo, M., and Sharifzadeh, M. (2017). Real time identification of automotive dry clutch frictional characteristics using trust region methods. In *AIMETA 2017 - Proceedings of the 23rd Conference of the Italian Association of Theoretical and Applied Mechanics*, volume 4, 526–534.

Sharifzadeh, M., Beglari, H., Chehrazad, S., and Akbari, A. (2016). Smart agricultural pumps control using realtime identification approach. *Patent No. 87709*.

Sharifzadeh, M., Farnam, A., Senatore, A., F., T., and Akbari, A. (2018). Delay-dependent criteria for robust lateral stability control of articulated vehicles. In *Advances in Service and Industrial Robotics*. Springer.

Sharifzadeh, M., Timpone, F., Senatore, A., Farnam, A., Akbari, A., and Russo, M. (2017). Real time tyre forces estimation for advanced vehicle control. *International Journal of Mechanics and Control*, 18(2), 77–84.

Terzo, M. and Timpone, F. (2013). The control of the handling of a front wheel drive vehicle by means of a magnetorheological differential. *International Review of Mechanical Engineering*, 7(3), 395–401.

Vasca, F., Iannelli, L., Senatore, A., and Reale, G. (2011). Torque transmissibility assessment for automotive dry-clutch engagement. *IEEE/ASME transactions on Mechatronics*, 16(3), 564–573.